

A facile solution-chemistry method for Cu(OH)₂ nanoribbon arrays with noticeable electrochemical hydrogen storage ability at room temperature†

Peng Gao,* Milin Zhang, Zhongyi Niu and Quanping Xiao

Received (in Cambridge, UK) 28th August 2007, Accepted 2nd October 2007

First published as an Advance Article on the web 12th October 2007

DOI: 10.1039/b713154b

Cu(OH)₂ nanoribbon arrays were synthesized by a simple room-temperature solution reaction for the first time, which exhibited noticeable hydrogen storage capacity and large BET surface area.

In recent years, the “chemistry of form” has attracted considerable interest in chemistry and materials science. One-dimensional (1D) nanoscaled materials such as carbon nanotubes (CNTs),¹ semiconductor nanowires and nanobelts² exhibit interesting and useful properties and may be applied as building blocks for the integration of the next generation of nanoelectronics, ultrasmall optical devices, biosensors, *etc.* A prerequisite for such integration is able to assemble the 1D nanomaterials in desired and functional structures. In the past, isotropic nanoparticles were used as building blocks of superlattices³ and 3-D microspheres.⁴ Also some techniques, such as DNA templates, biotin–streptavidin interaction, Langmuir–Blodgett technique, *etc.*, were employed to obtain ordered arrays of short nanorods.⁵ Among these methods, the solution-chemistry methods have potential advantages of relatively low cost, avoiding complicated processes, and special instruments. However, few researches have aimed at assembling inorganic 1-D nanostructures in solution.⁶ There is still a big challenge to the preparation of nanowire and nanobelt arrays through the solution-chemistry method at room temperature.

Recently, copper-based nanowires and nanobelts have received increasing attention because of their potential applications. Orthorhombic Cu(OH)₂ is a well-known layered material. The magnetic properties of Cu(OH)₂ are remarkably sensitive to the intercalation of molecular anions,⁷ making the material a candidate for sensor applications. Cu(OH)₂ nanowires have been used as precursors for the synthesis of Cu₂O nanowires.⁸ Up to now, the literature reported about synthesis of Cu(OH)₂ nanowires through a solution-phase approach is extremely sparse. Only in recent studies, Yang and co-workers reported that Cu(OH)₂

nanoribbons with a high aspect ratio were prepared by coordination self-assembly in solution,⁹ and dispersed Cu(OH)₂ and CuO nanoribbons were synthesized on a copper surface in a controlled fashion.¹⁰ Here, a new strategy has been applied to fabricate Cu(OH)₂ nanoribbon arrays through a simple room-temperature solution reaction, which indicates the importance of alkaline conditions to the building of the 1-D hydrate nano arrays.

In a typical experiment, 100 mL benzene was allowed to stand in contact with equal amount of an aqueous layer in a 500 mL beaker. The pH value of the aqueous layer was adjusted to 10 using 30% NH₃·H₂O solution. Then a pure copper foil (0.02 × 1 × 10 cm), which was washed with dilute acetic acid and distilled water several times and sonicated in acetone for 5 min, was vertically immersed in the solution. After that 10 mL Cu(CH₃COO)₂ solution (1 M) was added slowly into the system. Finally, the solution was kept at room temperature for 24 h. All the steps above were carried out without any stirring. Finally the foil was washed with distilled water and absolute ethanol several times.

The overall crystallinity and purity of the as-synthesized sample were examined by XRD measurements performed on a Rigaku X-ray diffractometer with Cu-Kα radiation. All of the diffraction peaks in Fig. 1(d) can be readily indexed to a pure orthorhombic phase (space group: *Cmc*2₁) with lattice constants *a* = 2.96 Å, *b* = 10.55 Å and *c* = 5.26 Å, which is in good agreement with the literature values for bulk orthorhombic Cu(OH)₂ (JCPDS 13-0420). The other peaks are all due to the copper substrate. In

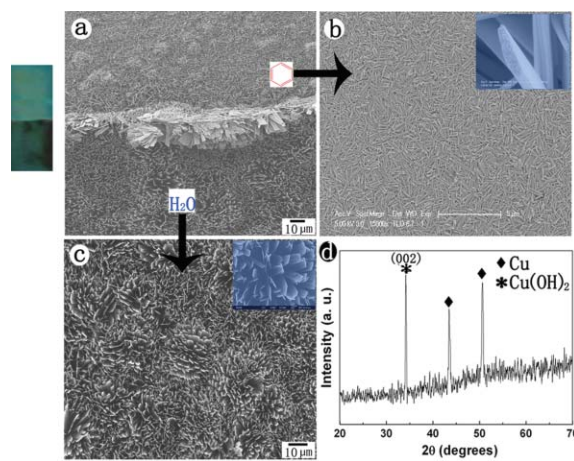


Fig. 1 (a), (b) and (c): FE-SEM images of Cu(OH)₂ nanoribbons prepared in the benzene/NH₃·H₂O system; (d) XRD pattern of copper foil obtained in the NH₃·H₂O layer.

Key Laboratory of Superlight Materials and Surface Technology, Ministry of Education, Harbin Engineering University, Harbin, Heilongjiang, 150001, P. R. China. E-mail: gaopeng@hrbeu.edu.cn; Fax: +86-451-82519696; Tel: +86-451-82519696;

† Electronic supplementary information (ESI) available: Fig. S1: Schematic showing the coordination assembly growth of Cu(OH)₂ nanoribbons. Fig. S2: SEM image of the Cu(OH)₂ nanowires prepared only in NH₃·H₂O solutions. Fig. S3: N₂ adsorption–desorption isotherm of the as-obtained Cu(OH)₂ nanoribbon arrays; inset, pore-size distribution curve obtained from the desorption data. Fig. S4: High magnification FE-SEM image of the boundary between the water layer and benzene layer. Fig. S5: FE-SEM image of the Cu(OH)₂ nanoribbon arrays after being cycled 50 times at a charge–discharge current density of 10 mA g⁻¹. See DOI: 10.1039/b713154b

addition, it is found that peak (002) is the only peak that showed a substantial increase in relative intensity, indicating that the ribbon growth may occur along the (002) plane.

After an aging time of 24 h, $\text{Cu}(\text{OH})_2$ ribbons were formed. Examination by FE-SEM revealed that the products in both the $\text{NH}_3 \cdot \text{H}_2\text{O}$ layer and benzene layer are primarily composed of ribbons with lengths of up to several micrometers (Fig. 1(b) and (c)). Most of the ribbons are straight and uniform along their axis direction. A clear boundary can be seen in Fig. 1(a) which divides the lying ribbons formed in the benzene layer from the standing ones formed in the aqueous layer. Interestingly, it was also found that each ribbon was made up of smaller ribbons with the same length (Fig. 2(a)), which has never been found in previous literature. Even though the sample was subjected to strong ultrasonic treatment, it still maintained a bundle-like morphology (Fig. 2(b)). Further details about the structure of the ribbons were investigated by the SAED pattern and HRTEM. The SAED image (Fig. 2(c)) taken from the ribbon indicated in Fig. 2(b) can be indexed as a orthorhombic $\text{Cu}(\text{OH})_2$ single crystal, in good agreement with the XRD results presented above. Moreover, the SEAD images taken from different positions along the ribbon (without tilting the sample with respect to the electron beam) were found to be almost identical.

This indicates that the entire ribbon is a single crystal, which is different from the $\text{Cu}(\text{OH})_2$ nanowires synthesized in analogous aqueous–organic interfaces.¹¹ Fig. 2(d), showing a typical HRTEM image, reveals that the ribbon is structurally uniform with a clear inter-planar spacing of about 2.63 Å, which corresponds to (002) planes. In addition, the (002) planes are parallel to the axis of the ribbon, indicating that the ribbons grow along the (002) planes, which is consistent with the observations from the XRD image.

The primary reaction in the preparation of $\text{Cu}(\text{OH})_2$ nanoribbons through this liquid–solid–solution (LSS) process involved the reaction of Cu^{2+} ions and OH^- ions at the interface of the $\text{NH}_3 \cdot \text{H}_2\text{O}$ and benzene layer (solid), benzene liquid phase (liquid) and $\text{NH}_3 \cdot \text{H}_2\text{O}$ solutions (solution). There are two reasons guiding

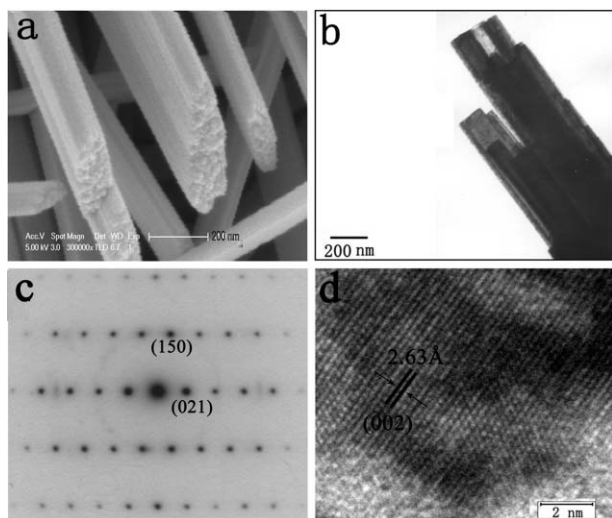


Fig. 2 (a) FE-SEM image of $\text{Cu}(\text{OH})_2$ nanoribbons; (b) TEM image of the products after strong ultrasonic treatment; (c) SAED pattern and (d) HRTEM image of a single nanoribbon.

us in selecting this system. One is that $\text{Cu}(\text{OH})_2$ is a layered material with orthorhombic crystal structure, and under the right conditions, the crystal growth rate is expected to be quite different.¹² The other is that Cu^{2+} prefers square planar coordination by OH^- in $\text{NH}_3 \cdot \text{H}_2\text{O}$ solutions through the action of OH^- to d_{z^2} of Cu^{2+} , forming a two-dimensional (2D) structure (see ESI†), which has been proved critical for the formation of $\text{Cu}(\text{OH})_2$ nanoribbons.¹³ This special 2D structure also provides the possibility for standing up of the nanoribbons. It is well known that the atoms at the bulk metal surface usually exhibit a positive charge, and in the alkaline solution OH^- ions will tend to adsorb on the metal surface. In the suitable weak alkaline conditions with lower concentration of Cu^{2+} ions, the OH^- ions on the metal surface will promote $\text{Cu}(\text{OH})_2$ nuclei mainly forming on the surface of the substrate. Because the end of the copper substrate in the $\text{NH}_3 \cdot \text{H}_2\text{O}$ solutions absorbed by many OH^- ions is electropositive, the other electronegative end will repulse the $\text{Cu}(\text{OH})_4^{2-}$, which is unfavorable to the 1D orientated growth. This may be the reason why the nanoribbons formed in the benzene layer lie down on the copper substrate.

Comparison of the morphology of $\text{Cu}(\text{OH})_2$ obtained in $\text{NH}_3 \cdot \text{H}_2\text{O}$ solutions and at the benzene/ $\text{NH}_3 \cdot \text{H}_2\text{O}$ interface has also been made (see ESI†). In the sediments of sample A, a large number of $\text{Cu}(\text{OH})_2$ nanowires, lying together yet parallel to the copper substrate, were abundantly obtained. It is known that the nucleation rate of $\text{Cu}(\text{OH})_2$ at the interface in the organic phase/aqueous phase will be slowed,¹¹ which was helpful for the formation of $\text{Cu}(\text{OH})_2$ nanoribbons. The concentration of OH^- ions also obviously affected the formation of $\text{Cu}(\text{OH})_2$ nanoribbons. Comparison experiments with different pH values (pH = 9–14) while keeping other synthetic parameters unchanged leads to a dramatic change in the size and shape of these particles, as shown in Fig. 3.

The porous nature of the nanoribbon arrays was further confirmed by a BJH measurement on a OMNISORP-100CX accelerated surface area and porosimetry system (see ESI†). The measurement shows that the BET surface area is $23.66 \text{ m}^2 \text{ g}^{-1}$ and the average pore diameter is 4.0 nm, which implies that the $\text{Cu}(\text{OH})_2$ nanoribbon arrays obtained here are mesoporous. Interestingly, the electrochemical study demonstrated that the

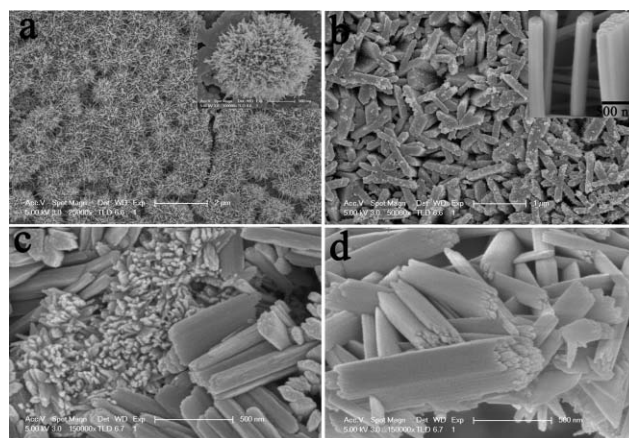


Fig. 3 FE-SEM images of the products obtained in aqueous layers with different pH value while keeping other synthetic parameters unchanged: (a) pH = 9, (b) pH = 11, (c) pH = 12, (d) pH = 14.

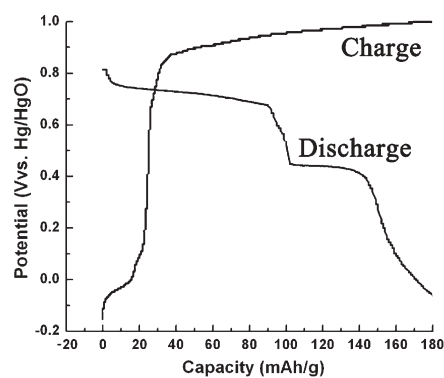


Fig. 4 Charge-discharge curves of $\text{Cu}(\text{OH})_2$ nanoribbon arrays at a constant current density of 10 mA g^{-1} .

discharge capacity of the $\text{Cu}(\text{OH})_2$ nanoribbon arrays displayed a noticeable electrochemical hydrogen storage ability, as shown in Fig. 4, which amounts to a hydrogen storage capacity of 0.5 wt% in SWNTs.¹⁴ In the charge curve of $\text{Cu}(\text{OH})_2$ nanoribbon arrays, one weak and perceptible voltage plateau is seen at ca. 3 mAh g^{-1} . With the increase of the electrochemical capacity, the potential increases quickly, but remains unchanged when the charge capacity reaches 18 mAh g^{-1} . One new obvious plateau of potential is observed between 38 and 180 mAh g^{-1} . This indicates that two different hydrogen adsorption sites^{14d} exist in the synthesized $\text{Cu}(\text{OH})_2$ nanoribbon arrays, in other words, there are two different electrochemical steps in the charging process. It is assumed that the H is first adsorbed into the smaller pores in each nanoribbon, which is made up of smaller ribbons (Fig. 2(a)), and then diffused into the interstitial sites among $\text{Cu}(\text{OH})_2$. After being cycled 50 times at a charge-discharge current density of 10 mA g^{-1} , the discharging capacities of the $\text{Cu}(\text{OH})_2$ nanoribbon arrays remains $>130 \text{ mAh g}^{-1}$. This indicates that the as-prepared $\text{Cu}(\text{OH})_2$ products have a strong resistance against oxidation and corrosion. After the measurement, the morphology of the product was unchanged (see ESI†).

In general, orthorhombic $\text{Cu}(\text{OH})_2$ is unstable because oxygen atoms are either pentacoordinated or tricoordinated. Its 1D nanostructures can be easily transformed to 1D CuO , CuO_2 and Cu nanoarrays under certain reaction conditions such as through heat treatment.^{11a} The nanoribbon arrays obtained here may be ideal precursors for preparing 1D copper(I) compounds, which is currently under investigation.

In summary, $\text{Cu}(\text{OH})_2$ nanoribbon arrays were synthesized by a simple room-temperature solution reaction for the first time. The products exhibit noticeable hydrogen storage capacity and large BET surface area. The present work shows that the nanostructures of the products are important to their electrochemical hydrogen storage performances. Further research will be performed on further novel copper 1D nanoarrays exhibiting different electrochemical hydrogen storage performances, for which superior hydrogen storage materials might be found.

This research is supported by the Natural Science Foundation of China (No. 50772025).

Notes and references

- 1 S. Iijima, *Nature*, 1991, **354**, 56.
- 2 (a) Y. Xia and P. Yang, *Adv. Mater.*, 2003, **15**, 351; (b) X. D. Wang, P. X. Gao, J. Li, C. J. Summers and Z. L. Wang, *Adv. Mater.*, 2002, **14**, 1732; (c) C. Ma, D. Moore, J. Li and Z. L. Wang, *Adv. Mater.*, 2003, **15**, 228.
- 3 (a) R. P. Andres, J. D. Bielefeld, J. I. Henderson, D. B. Janes, V. R. Kolagunta, C. P. Kubiak, W. J. Mahoney and R. G. Osifchin, *Science*, 1996, **273**, 1690; (b) M. Li, H. Schnablegger and S. Mann, *Nature*, 1999, **402**, 393.
- 4 (a) A. K. Boal, F. Ilhan, J. E. DeRouchey, T. Thurn-Albrecht, T. P. Russell and V. M. Rotello, *Nature*, 2000, **404**, 746; (b) J. Jin, T. Iyoda, C. Cao, Y. Song, L. Jiang, T. J. Li and D. B. Zhu, *Angew. Chem., Int. Ed.*, 2001, **40**, 2135.
- 5 (a) E. Dujardin, L. B. Hsin, C. R. C. Wang and S. Mann, *Chem. Commun.*, 2001, 1264; (b) K. K. Caswell, J. N. Wilson, U. H. F. Bunz and C. J. Murphy, *J. Am. Chem. Soc.*, 2003, **125**, 13914; (c) F. Kim, S. Kwan, J. Akana and P. D. Yang, *J. Am. Chem. Soc.*, 2001, **123**, 4360.
- 6 (a) N. Kimizuka, *Adv. Mater.*, 2000, **12**, 1461; (b) B. Messer, J. H. Song and P. Yang, *J. Am. Chem. Soc.*, 2000, **122**, 10232.
- 7 W. Fujita and K. Awaga, *J. Am. Chem. Soc.*, 1997, **119**, 4563.
- 8 W. Z. Wang, G. H. Wang, X. S. Wang, R. J. Zhang, Y. K. Liu and C. L. Zheng, *Adv. Mater.*, 2002, **14**, 67.
- 9 X. G. Wen, W. X. Zhang, S. H. Yang, Z. R. Dai and Z. L. Wang, *Nano Lett.*, 2002, **2**, 1397.
- 10 X. G. Wen, W. X. Zhang and S. H. Yang, *Langmuir*, 2003, **19**, 5898.
- 11 (a) Z. L. Wang and X. Y. Kong, *J. Phys. Chem. B*, 2003, **107**, 8275; (b) X. Y. Song, S. X. Sun, W. M. Zhang, H. Y. Yu and W. L. Fan, *J. Phys. Chem. B*, 2004, **108**, 5200.
- 12 R. R. Clemente, C. J. Serna, M. Ocana and E. Matijevic, *J. Cryst. Growth*, 1994, **143**, 277.
- 13 X. G. Wen, W. X. Zhang and S. H. Yang, *Nano Lett.*, 2002, **2**, 1397.
- 14 (a) J. Chen, N. Kuriyama, H. Yuan, H. T. Takeshita and T. Sakai, *J. Am. Chem. Soc.*, 2001, **123**, 11813; (b) X. Chen, X. P. Gao, H. Zhang, Z. Zhou, W. K. Hu, G. L. Pan, H. Y. Zhu, T. Y. Yan and D. Y. Song, *J. Phys. Chem. B*, 2005, **109**, 11525; (c) G. P. Dai, M. Liu, D. M. Cheng, P. X. Hou, Y. Tong and H. M. Chen, *Electrochem. Solid-State Lett.*, 2002, **5**, 13.